# Supporting Information

# Reaction Acceleration at the Surface of a Levitated Droplet by Vapor Dosing from a Partner Droplet

Lingqi Qiu, Xilai Li, Dylan T. Holden and R. Graham Cooks*

Department of Chemistry, Purdue University, West Lafayette, IN 47907, USA
E-mail: cooks@purdue.edu

# Table of Contents

# 1. General experimental section

## 1.1 Chemicals and materials

2,4,6-Triphenylpyrylium tetrafluoroborate (TPP, **1**), 1-methyl-2,4,6-triphenylpyridinium tetrafluoroborate (internal standard 1, **IS1**), and 4-formyl-1-methylpyridinium benzenesulfonate (FMPB) were purchased from Sigma Aldrich (St. Louis, MO). Triethylmethylammonium chloride (internal standard 2, **IS2**) and HPLC-grade acetonitrile were obtained from Fisher Scientific (Hampton, NH). All amines used in this study were sourced from Sigma Aldrich, Fisher Scientific, and Oakwood Chemicals (Hong Kong, China).

Borosilica glass capillaries for nanoelectrospray ionization mass spectrometry (nESI-MS) analysis, with dimensions of 1.5 mm O.D., 0.86 mm I.D., and 10 cm in length, were acquired from Sutter Instruments (Novato, CA).

The acoustic levitator kit was purchased from Makerfabs (Shenzhen, China) and fitted with custom electronics.

## 1.2 Instruments

All samples were analyzed by nESI coupled with a Finnigan LTQ linear ion trap mass spectrometer (ThermoFisher Scientific, San Jose, CA). In each case, a 5 µm internal diameter nESI emitter was prepared using P-97 Micropipette Puller (Novato, CA) and placed within a stainless-steel electrode. Positive or negative 2 kV spray voltage was applied, and a 5 mm spray distance between the sprayer tip and MS inlet was maintained. Other instrumental parameters included MS inlet temperature of 250 ºC, capillary voltage of 15 V, and tube lens of 65 V. Tandem mass spectrometry (MS/MS) was used for structural characterization of specific precursor ions.

The acoustic levitator was built and connected to a Tekpower TP-3005D-3 DC power supply to control the levitation voltage. For two-droplet levitation experiments, 13 V was applied in most cases, except for neopentylamine and sec-butylamine, where 12 V was applied. The distance between the two droplets was maintained at roughly 4 mm.

A handheld UV lamp purchased from Spectroline (Melville, New York) was used to generate light at a wavelength of 365 nm.

## 1.3 Experimental process for Vapor-dosing from a partner droplet

### 1.3.1   Procedure A: Limited amine dosing

Two droplets, consisting of a reacting droplet containing TPP and 2 µM **IS1** in acetonitrile solution (gold droplet in Fig. S1) and an amine reservoir droplet (blue droplet in Fig. S1), were pipetted and trapped in the acoustic levitator at different positions. After a dosing time of 3 or 5 seconds, the amine droplet was removed, and the reacting droplet was held inside the levitator for further reaction. After the desired reaction time, the entire droplet was collected and diluted fivefold with acetonitrile. This sample was analyzed by nESI-MS.
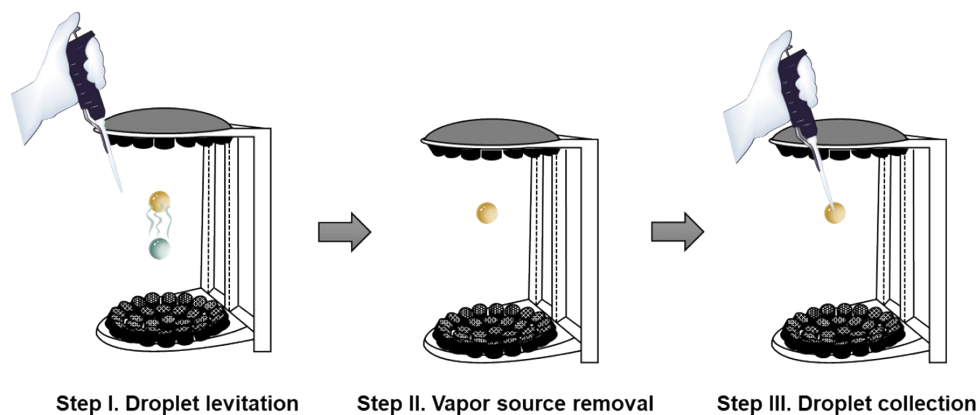
**Step I. Droplet levitation**     **Step II. Vapor source removal**     **Step III. Droplet collection**

Figure S1. Illustration of process for vapor-dosing experiment with limited dosing time.

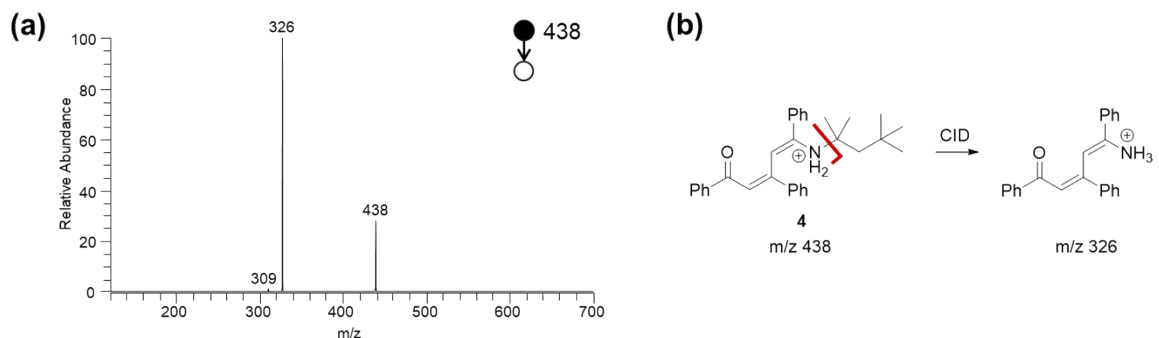### 1.3.2    Procedure B: Continuous amine dosing

Referring to *"condition a"* mentioned in Scheme 1 of the main text, two droplets, consisting of a reacting droplet containing 0.5 mM of TPP in acetonitrile and an amine reservoir droplet, were deposited and trapped in the acoustic levitator. After 1 minute, the reacting droplet was collected and diluted with 20 uL of acetonitrile for analysis.

Referring to *"condition b"* mentioned in Scheme 1 of the main text, after the one-minute vapor-dosed droplet reaction described in condition a, the amine droplet was removed, and 3 µL of 3% acetic acid in acetonitrile was directly added to the reacting droplet. After another minute, this reacting droplet was collected and diluted with 20 µL of acetonitrile for analysis.

Note that in the practical application of this two-droplet system in pyridinium synthesis, the concentration of TPP can be increased as needed.
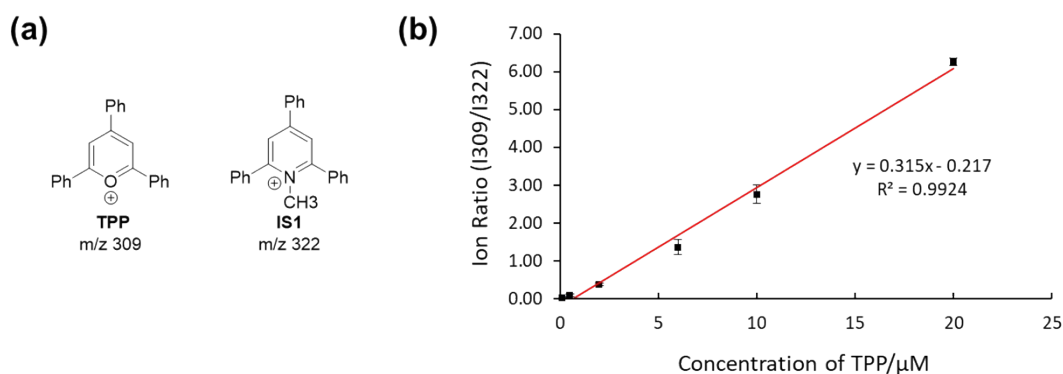
## 2. Mechanistic investigation of reaction acceleration observed in a vapor-dosed droplet

### 2.1 MS/MS analysis of product in model reaction



Figure S2. MS/MS analysis of the product observed in model reaction (a) MS$^2$ spectrum of the precursor ion at *m/z* 438 at CID 20. (b) Proposed fragmentation pathway, generating the productor ion at *m/z* 326.

### 2.2 Quantitation of TPP concentration

TPP solutions, ranging from 0.1 to 20 µM, were quantified using 2 µM **IS1**. All samples were prepared by mixing the target TPP solution with 4 µM **IS1** in a 1:1 (*v/v*) ratio. The resulting mixture was diluted fivefold with acetonitrile for nESI-MS analysis, and the ion abundance ratio between TPP (*m/z* 309) and **IS1** (*m/z* 322) was used to establish the calibration curve (Fig. S3) and quantify the TPP in reaction mixtures.



Figure S3. TPP quantitation using **IS1** as internal standard. (a) Structure of TPP and **IS1**. (b) Calibration curve of 0.1 to 20 µM TPP, with three replicates in each case. All solutions were prepared in acetonitrile.

### 2.3 Quantitation of dosed amine in reacting droplet

#### 2.3.1   Calibration equation used for quantitative amine measurement

The tert-octylamine solutions, ranging from 1 to 10 mM, were quantified using 5 mM **IS2**. All samples were prepared by mixing the amine solution with 10 mM **IS2** in a 1:1 (v/v) ratio. The resulting mixture was diluted fivefold with a solution of 1% acetic acid in acetonitrile for nESI-MS analysis, and the ion abundance ratio between protonated amine (m/z 130) and **IS2** (m/z 116) was used to establish the calibration curve (Fig. S4) and to quantify the amine captured in the vapor-dosed droplet (see section 2.3.2).
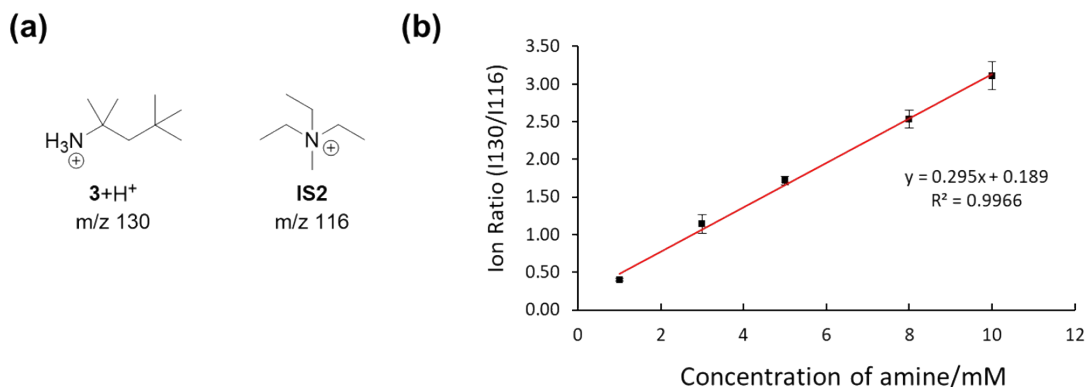
Figure S4. Tert-octylamine quantitation using **IS2** as internal standard. (a) Structure of protonated **3** and **IS2**. (b) Calibration curve of 1 to 10 mM **3**, with three replicates in each case. All the initial amine and **IS2** solutions were prepared in acetonitrile.

### 2.3.2 Measurement of amine in reacting droplet captured from its partner droplet

Two droplets, consisting of a capturing acetonitrile droplet and a liquid amine reservoir droplet, were trapped in the acoustic levitator. After a dosing time of 3 or 5 seconds, the capturing droplet was collected, followed by the same sample preparation and detection process described in 2.3.1. The results for 3-second and 5-second dosing are displayed in Tables S1 and S2 (five replicates each), showing an average amine concentration in the capturing droplet of 2.2 mM and 4.8 mM, respectively.

Table S1. Captured amine concentration under 3-second dosing

| Replicates | R1 | R2 | R3 | R4 | R5 | Average |
|---|---|---|---|---|---|---|
| Captured amine/mM | 2.2 | 1.6 | 2.5 | 1.9 | 2.8 | **2.2** |

Table S2. Captured amine concentration under 5-second dosing

| Replicates | R1 | R2 | R3 | R4 | R5 | Average |
|---|---|---|---|---|---|---|
| Captured amine/mM | 3.8 | 6.9 | 3.8 | 5.5 | 4.0 | **4.8** |

### 2.3.3 Calculation of saturated concentration in surface region of amine **3** in vapor-dosed droplet

In the surface reaction control region (when [TPP] is lower than 5 µM), the droplet reaction presumably follows pseudo zero-order kinetics in both vapor-dosed and homogeneous droplets (Fig. 3b and 3c). Given the identical TPP distribution but distinctive amine distribution in these two cases, the expressions for surface reaction rate for the vapor-dosed droplet (Equation 1) and the homogeneous droplet (Equation 2) are as follows, where $Rate_s$, $k_s$, $[TPP]_s$, $[Amine]_s$, and $[amine]$ represent the surface rate, the surface rate constant, surface-saturated TPP concentration, surface-saturated amine concentration in vapor-dosed droplet, and surface concentration of amine in the homogeneous droplet, respectively. Note that in the homogeneous droplet, the amine is evenly distributed; therefore, the amine concentration at the surface is assumed to be the same as the reservoir amine concentration (which also equals the core concentration).

$$Rate_s = k_s \cdot [TPP]_s [Amine]_s \dotfill (1)$$

$$Rate_s = k_s \cdot [TPP]_s[Amine] \quad\text{............................................................(2)}$$

Considering that the kinetics shown in Fig. 3b and 3c were obtained by sampling and analyzing the entire droplets, the measured reaction rates — viz. the slopes in Fig. 3b and 3c — are global reaction rates. Although the surface reaction makes the major contribution, the overall reaction rate is diluted by the total droplet volume. This relationship can be expressed as Equation 3, where *Rate*, *V*, and $V_s$ represent the global reaction rate, the volume of the entire droplet, and the volume of the surface region, respectively.

$$Rate \cdot V = Rate_s \cdot V_s \quad\text{..........................................................(3)}$$

By combining Equation 1 or Equation 2 with Equation 3, the relationship between the surface reaction parameters and experimental results can be established as Equations 4 and 5, depicting the scenarios in vapor-dosed and homogeneous droplets, respectively.

$$Rate = \frac{V_s}{V} \cdot k_s \cdot [TPP]_s[Amine]_s \quad\text{.......................................................(4)}$$

$$Rate = \frac{V_s}{V} \cdot k_s \cdot [TPP]_s[Amine] \quad\text{.......................................................(5)}$$

Given the identical droplet size and TPP concentrations and distributions in these two systems, *V*, *V*, $V_s$, $k_s$, *[TPP]$_s$*, will be the same. As a result, *[Amine]$_s$* can be readily calculated using Equation 6, derived by dividing Equation 4 by Equation 5.

$$\frac{Rate_{vapor-dosed}}{Rate_{homogeneous}} = \frac{[Amine]_s}{[Amine]} \quad\text{.............................................................(6)}$$

The experimental results and the calculated *[Amine]$_s$* concentrations are displayed in Table S3. Note that the slope in each case represents the global reaction rate, *Rate.*

Table S3. Calculation of [Amine]s in vapor-dosed droplet

| Conditions | Corresponding amine concentration ([Amine]) | Slope (vapor-dosed droplet) | Slope (homogeneous droplet) | [Amine]$_s$ |
|---|---|---|---|---|
| 3-second dosing | 2 mM | -0.17 µM·s$^{-1}$ | -0.038 µM·s$^{-1}$ | 9 mM |
| 5-second dosing | 5 mM | -0.18 µM·s$^{-1}$ | -0.082 µM·s$^{-1}$ | 11 mM |

## 2.4 Near-surface sampling of levitated droplet

Two different types of glass capillary tips were used to sample the near-surface or interior regions. Note that the inner diameter of both tips was 40 µm, but their shapes differed. The interior sampling approach (Fig. S5c and S5d) used a tip with a long taper to pierce the droplet, while the near-surface sampling approach (Fig. S5a and S5b) used a tip with a short taper. The shorter taper tip causes the

droplet to quickly deform and attach to the outside of the tip when it touches the droplet surface, terminating the sampling procedure. Therefore, only the regions at or near the droplet surface are collected.
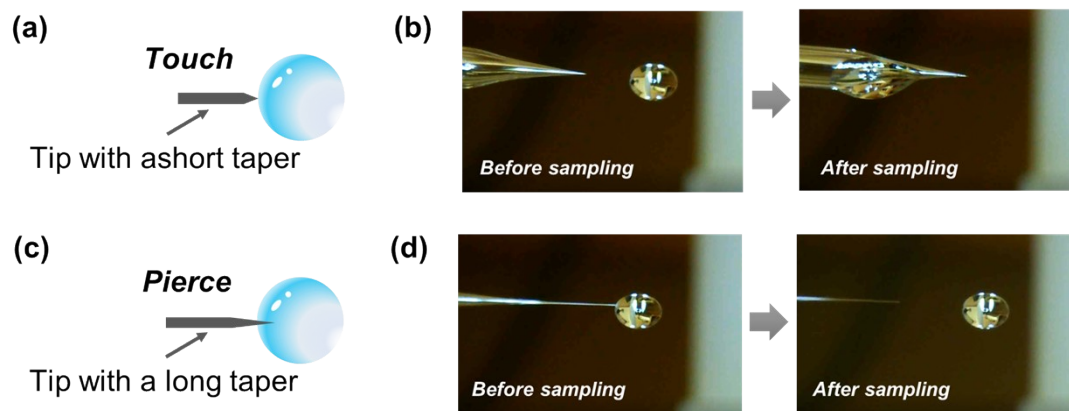


Figure S5. Near surface vs. interior region sampling of a levitated droplet. (a) Near-surface sampling strategy by using a tip with a short taper. (b) When the droplet touches the tip, it is immediately deformed and attached to the outer wall of the tip, naturally controlling the sampling region to the surface and near surface. (c) Interior sampling method by using a tip with a long taper. (d) This tip pierces the droplet and samples its interior region.

The near-surface sampling of a 3 µL levitated TPP droplet (initial concentration of TPP was 5 µM) was performed using the tip with a short taper. After sampling, the sampled volume was determined under a microscope. Subsequently, 3 µL of acetonitrile was added to the same tip to provide enough sample for nESI-MS analysis but at decreased TPP concentration. Six replicates were obtained, and the measured sampling volume from the levitated droplet is summarized in Table S4. On average, the sampling volume was 0.0079 µL, indicating a dilution factor of about 380. Note that the "near-surface" sampled volume of 8 nL is much greater than the expected surface monolayer, which was just 0.01 nL ($10^{-5}$ µL).

Table S4. Sampled volume of TPP droplet

| Replicates | R1 | R2 | R3 | R4 | R5 | R6 |
|---|---|---|---|---|---|---|
| Height/µm | 450 | 400 | 450 | 450 | 450 | 450 |
| Radius 1/µm | 20 | 20 | 20 | 20 | 20 | 20 |
| Radius 2/µm | 100 | 100 | 100 | 100 | 150 | 150 |
| Volume/µL | 0.006 | 0.005 | 0.006 | 0.006 | 0.012 | 0.012 |

The diluted samples were further analyzed by nESI-MS. However, in no replicates was signal for TPP observed. The detection limit of TPP was determined by analyzing 10 nM and 100 nM TPP standard solutions under the same conditions. As shown in Fig. S6, the TPP signal is still detectable at 100 nM, implying that the concentration of TPP in the diluted sample is less than 100 nM. Given that the dilution factor is approximately 380, the surface region concentration of TPP is less than 38 µM. For this reason, the calculated value of the RAF represents a lower limit.
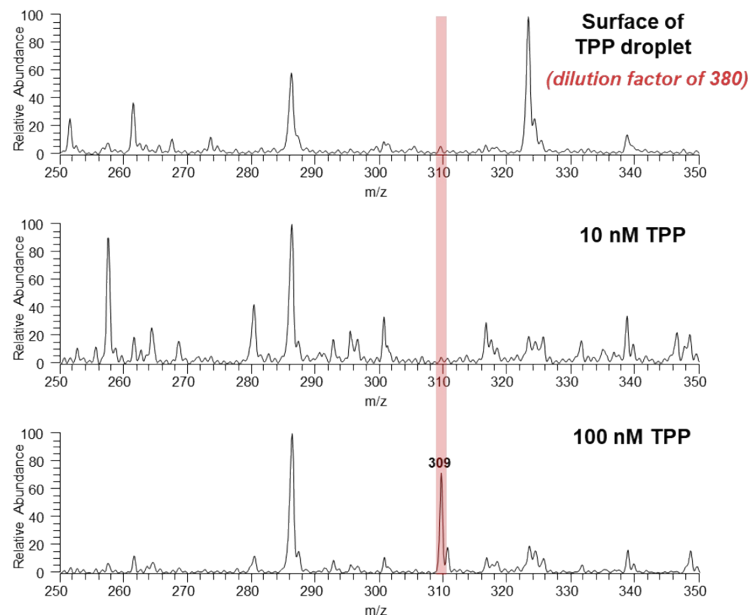
Figure S6. Comparison of mass spectra of sampled TPP at droplet surface (diluted with acetonitrile for detection), 10 nM TPP solution and 100 nM TPP solution.

## 2.5 Calculation of surface rate constant in vapor-dosed droplet

As mentioned in section 2.3.3, the relationship between the surface reaction parameters and experimental results for the vapor-dosed droplet in the surface reaction control region can be established as Equation 4, which can be readily rewritten as Equation 7:

$$Rate = \frac{V_s}{V} \cdot k_s \cdot [TPP]_s [Amine]_s \quad \text{......................................................} (4)$$

$$k_s = \frac{Rate \cdot V}{[Amine]_s \cdot [TPP]_s \cdot V_s} \text{.................................................................} (7)$$

From the previous calculation and estimation, the global reaction rate, *Rate,* was measured as 0.175 µM·s⁻¹ (average of two separate experiments with reaction rates of 0.17 µM·s⁻¹ and 0.18 µM·s⁻¹ ); the droplet volume, *V,* was 3 µL; *[Amine]$_s$* was calculated as 10 mM (average of two separate experiments with *[Amine]$_s$* of 9 mM and 11 mM); [TPP]$_s$ was measured as less than 38 µM; the volume of surface region, *Vs,* was estimated as $10^{-5}$ µL. By applying these values to Equation 7, $k_s$ can be readily calculated as more than $1.4 \times 10^5$ M⁻¹·s⁻¹.

## 2.6 Discussion on diffusion

The measured five orders of magnitude in acceleration at the droplet surface in this case is consistent with the RAF values often observed in micro-sized droplets, which corresponds to the overall reaction contribution (surface and core). In comparison, the RAF for the overall reaction in the vapor-dosed droplet is only 31, which is much lower than the RAF in microdroplets despite being exceptionally high for a millimeter-scale droplet. The small fraction of reagents entering the surface

region, where the reactions are accelerated, is presumably the main reason for the low RAF for overall reaction despite the high RAF for surface reaction. Clear evidence of diffusion of amine was seen in the amine-dosed droplet (Fig. S7). Note that even after 20 s the diffusion length is less than half of the droplet radius. This slow diffusion makes it difficult for the reagents to transfer from the surface to the center and vice versa. Consequently, in a large droplet, the reagents originally located in the interior region have a low chance of moving into the active region. Meanwhile, if the surface reaction is very fast, the diffusion rate becomes slower than the reaction rate, causing the reactants or products generated at surface to be "trapped" at the surface and occupy the active sites, leaving no available sites for further reagents. The scenario is different in the smaller ("microdroplets" of ESSI) where the diffusion length is comparable to the droplet size. Reagents can therefore move easily in microdroplets, and the surface of the droplet is thus refreshed, allowing for a greater fraction of reagents to dynamically occur the surface.
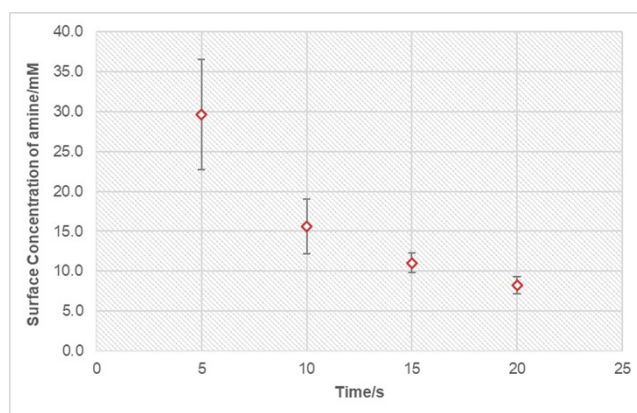


Figure S7.Near-surface concentration of amine in the vapor-dosed droplet (5-second dosing) showing changes over time. A surface sampling method (see section 2.4 for details) was applied, and internal standard 2 (**IS2**) was added to quantify the amine concentration.

### 2.7 Quantitation of water adsorption in levitated droplet

FMPB was used as a molecular probe to capture and quantify the water content in an acetonitrile droplet (Fig. S8a). The standard solutions were prepared by mixing acetonitrile with added water. Each standard solution was diluted fivefold with acetonitrile and then mixed with 1.6 mM FMPB in a ratio of 1:1 (*v/v*). A calibration curve was established by plotting the amount of added water in acetonitrile against the ion ratio of $[FMPB+H_2O]^+$ (*m/z* 140) and $[FMPB]^+$ (m/z 122) (Fig. S8b).
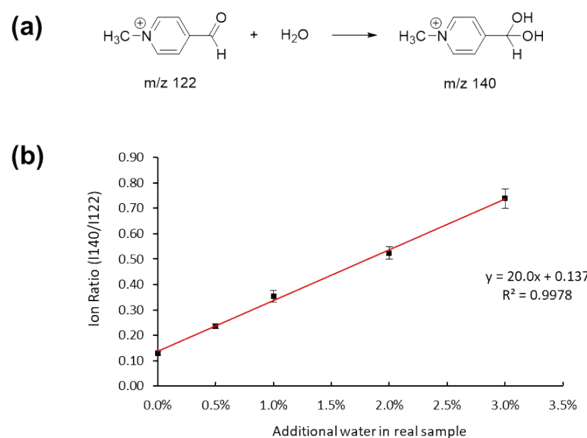
Figure S8. Quantitation of water using FMPB as a molecular mass tag. (a) Water adduct of FMPB. (b) Calibration curve of 0% to 3% additional water in acetonitrile, with three replicates in each case.

The water adsorption in a levitated acetonitrile droplet was quantified by collecting the 30-second levitated droplet, diluting it fivefold with acetonitrile, and mixing it with 1.6 mM FMPB solution in a ratio of 1:1 (*v/v*). On average, the measured additional water is 2.0% (amount shown in Table S5).

Table S5. Water adsorption after 30-second levitation

| Replicates | R1 | R2 | R3 | Average |
|---|---|---|---|---|
| Captured additional water | 1.8% | 1.9% | 2.1% | **2.0%** |

## 2.8 Effect of water adsorption in Katritzky reaction
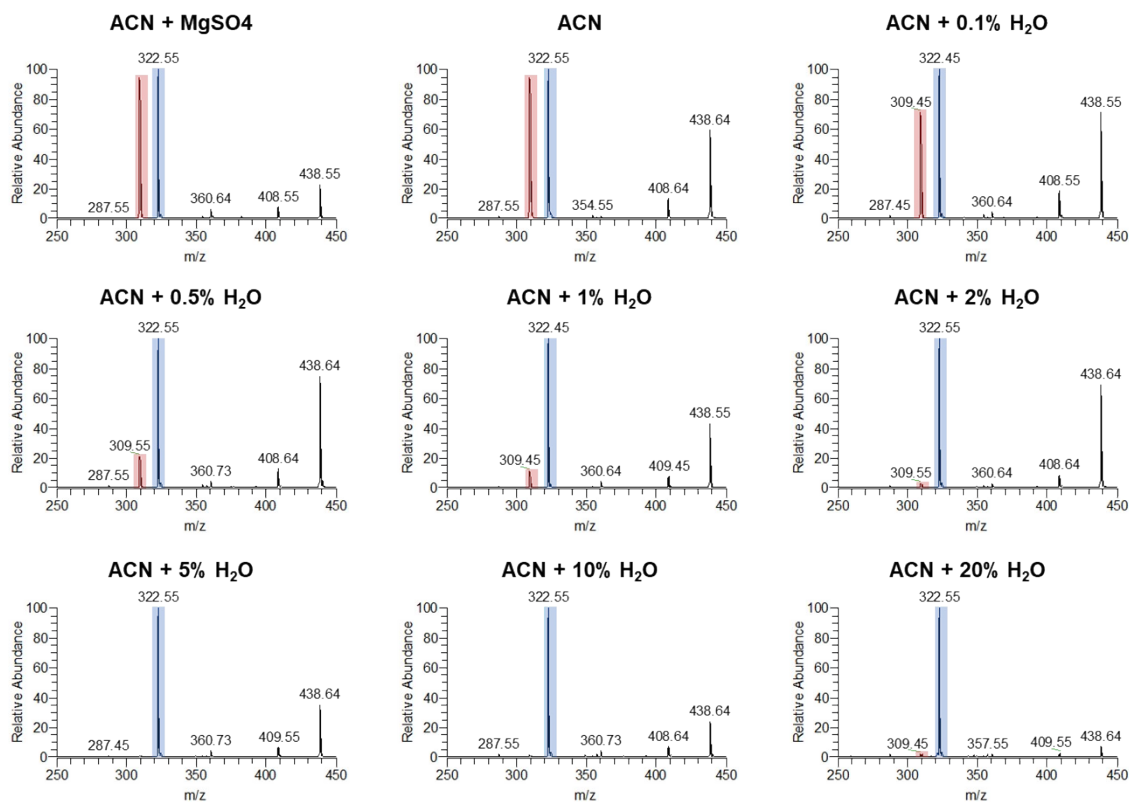


Figure S9. Water effect on Katritzky reaction in bulk (starting with 10 µM of TPP and 5 mM tert-octylamine). All the reaction products were analyzed after 2.5 minutes. The signal of TPP (reactant, at *m/z* 309) and **IS1** (internal standard, at *m/z* 322) are annotated as red and blue columns, respectively.
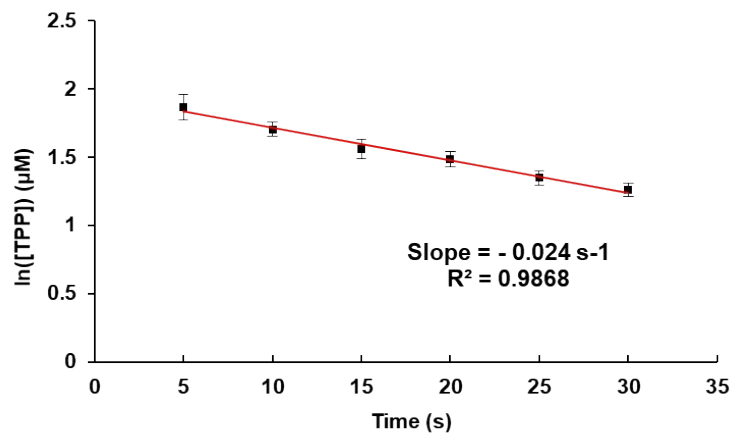
Figure S10. Kinetics in bulk with additional 2% water (starting with 10 μM of TPP and 5 mM tert-octylamine)

# 3. Substrate scope of Katritzky transamination in a vapor-dosed droplet
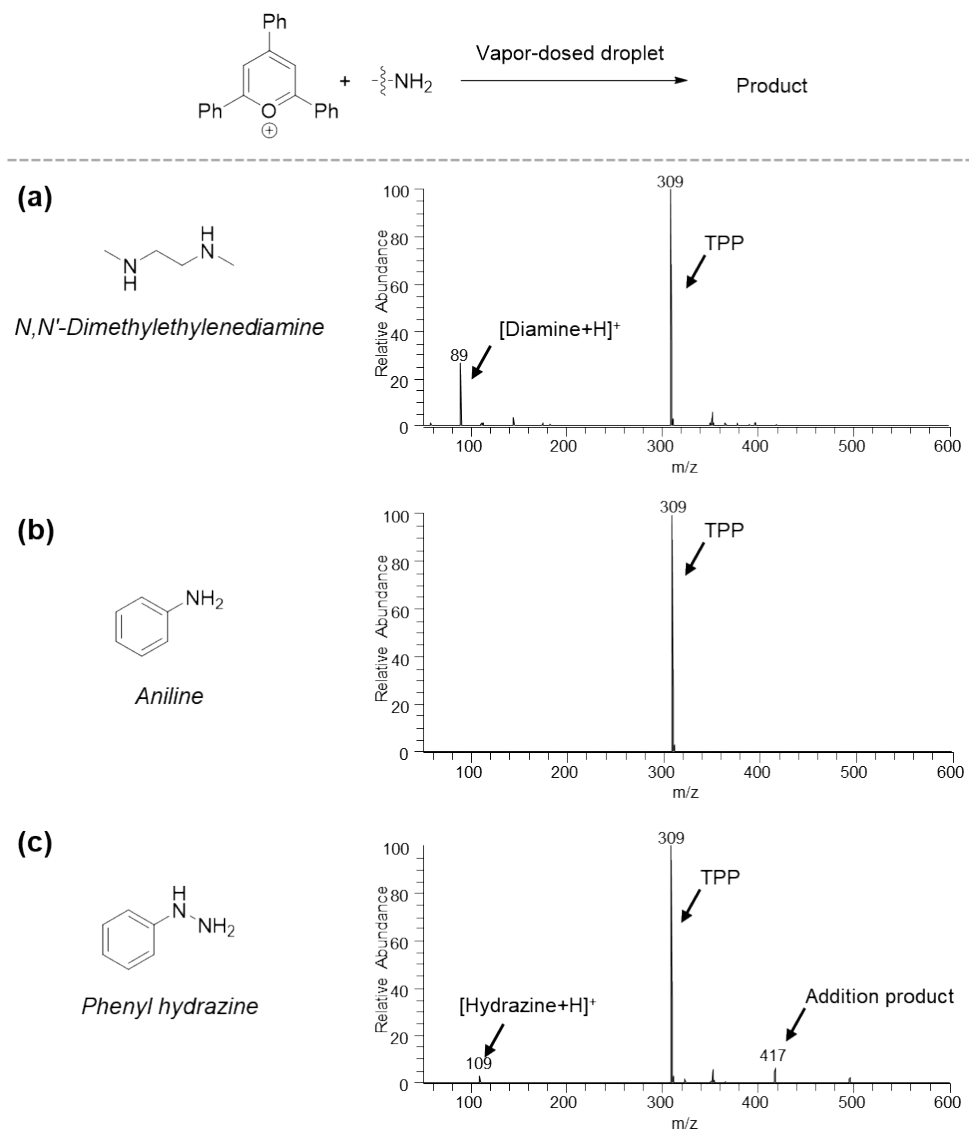


Figure S11. Reaction between TPP and (a) diamine, (b) aniline and (c) phenylhydrazine in levitated vapor-dosed droplet, under condition a.
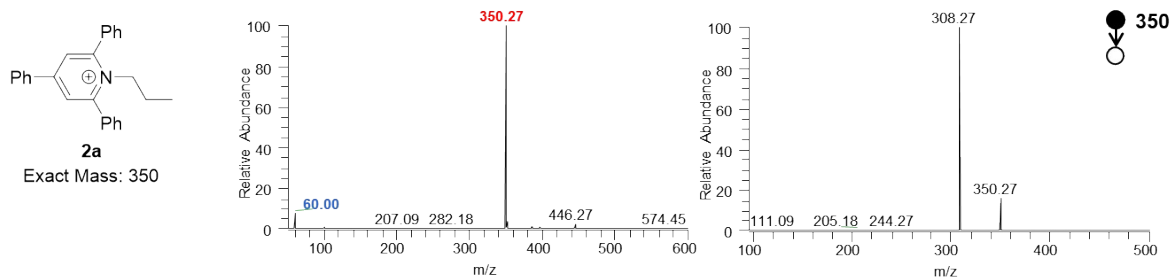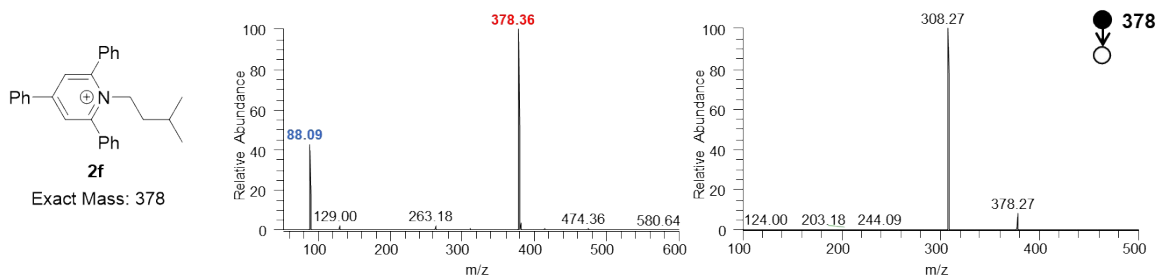
Figure S12. Mass spectrum illustrating the preparation of pyridinium **2a** under condition b (left panel). The signals for protonated amine **5a** and product **2a** are annotated in blue and red, respectively. The right panel shows the MS$^2$ spectrum of **2a** under CID 25.
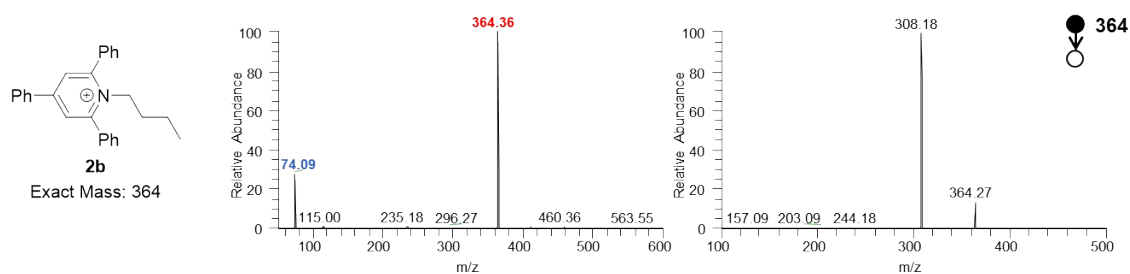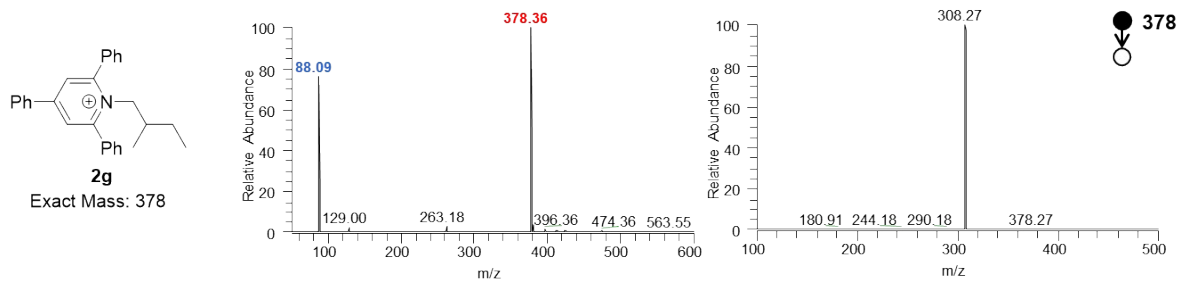


Figure S13. Mass spectrum illustrating the preparation of pyridinium **2b** under condition b (left panel). The signals for protonated amine **5b** and product **2b** are annotated in blue and red, respectively. The right panel shows the MS$^2$ spectrum of **2b** under CID 25.
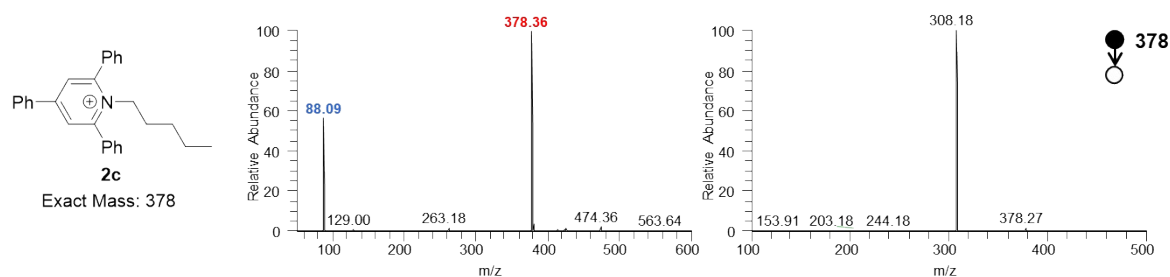


Figure S14. Mass spectrum illustrating the preparation of pyridinium **2c** under condition b (left panel). The signals for protonated amine **5c** and product **2c** are annotated in blue and red, respectively. The right panel shows the MS$^2$ spectrum of **2c** under CID 25.
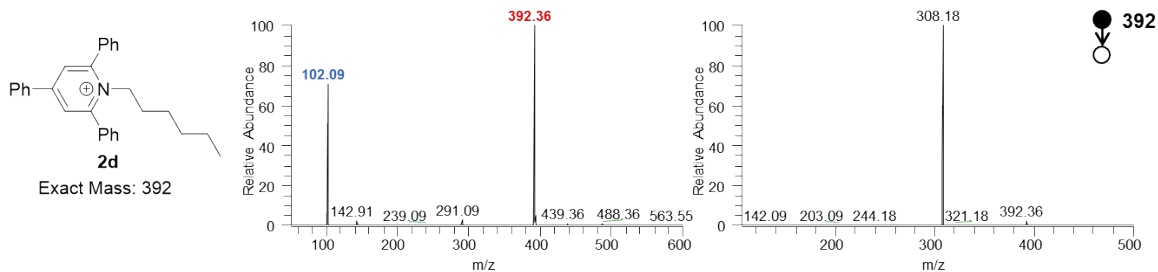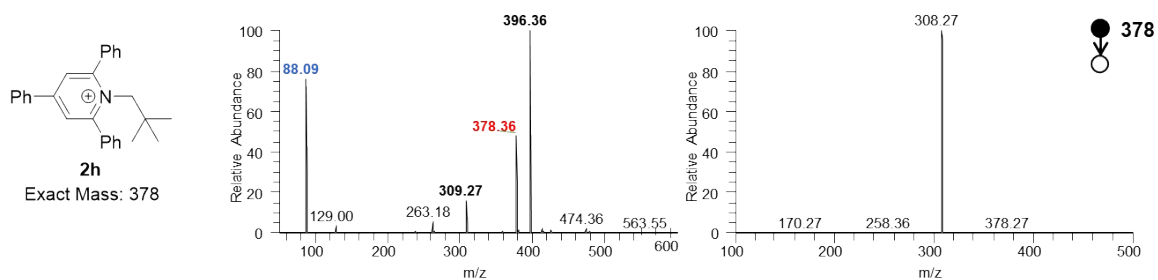
Figure S15. Mass spectrum illustrating the preparation of pyridinium **2d** under condition b (left panel). The signals for protonated amine **5d** and product **2d** are annotated in blue and red, respectively. The right panel shows the MS$^2$ spectrum of **2d** under CID 30.
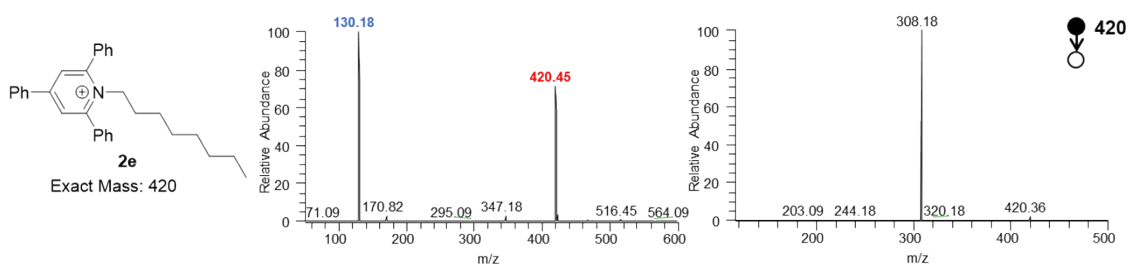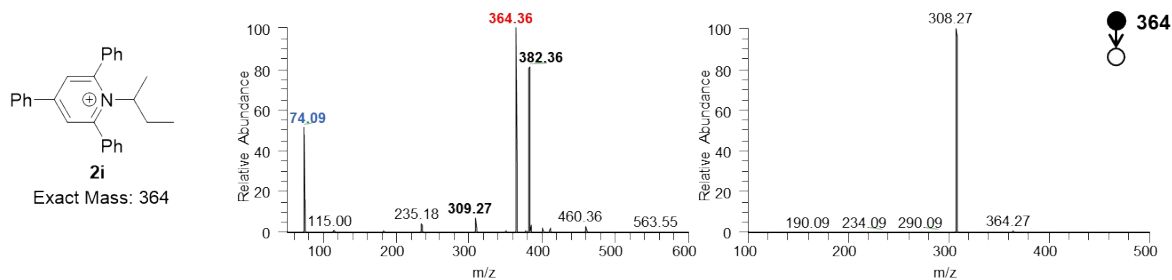


Figure S16. Mass spectrum illustrating the preparation of pyridinium **2e** under condition b (left panel). The signals for protonated amine **5e** and product **2e** are annotated in blue and red, respectively. The right panel shows the MS$^2$ spectrum of **2e** under CID 30.



Figure S17. Mass spectrum illustrating the preparation of pyridinium **2f** under condition b (left panel). The signals for protonated amine **5f** and product **2f** are annotated in blue and red, respectively. The right panel shows the MS$^2$ spectrum of **2f** under CID 25.
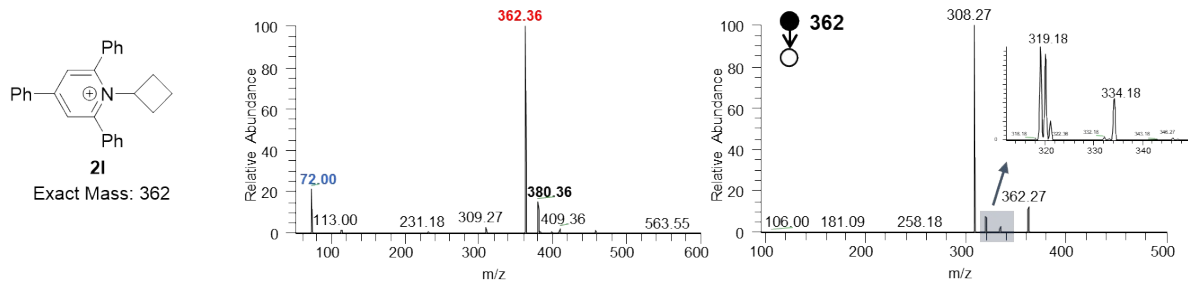
Figure S18. Mass spectrum illustrating the preparation of pyridinium **2g** under condition b (left panel). The signals for protonated amine **5g** and product **2g** are annotated in blue and red, respectively. The right panel shows the MS$^2$ spectrum of **2g** under CID 30.
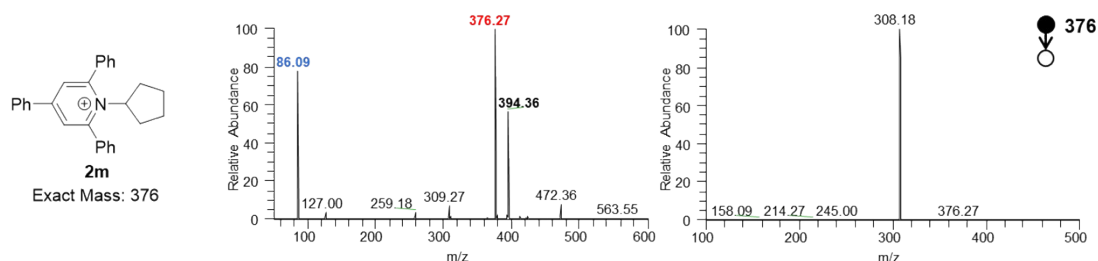


Figure S19. Mass spectrum illustrating the preparation of pyridinium **2h** under condition b (left panel). The signals for protonated amine **5h** and product **2h** are annotated in blue and red, respectively. The peaks at *m/z* 309 and 396 represent TPP and addition product **6h**, respectively. The right panel shows the MS$^2$ spectrum of **2h** under CID 25.



Figure S20. Mass spectrum illustrating the preparation of pyridinium **2i** under condition b (left panel). The signals for protonated amine **5i** and product **2i** are annotated in blue and red, respectively. The peaks at *m/z* 309 and 382 represent TPP and addition product **6i**, respectively. The right panel shows the MS$^2$ spectrum of **2i** under CID 25.
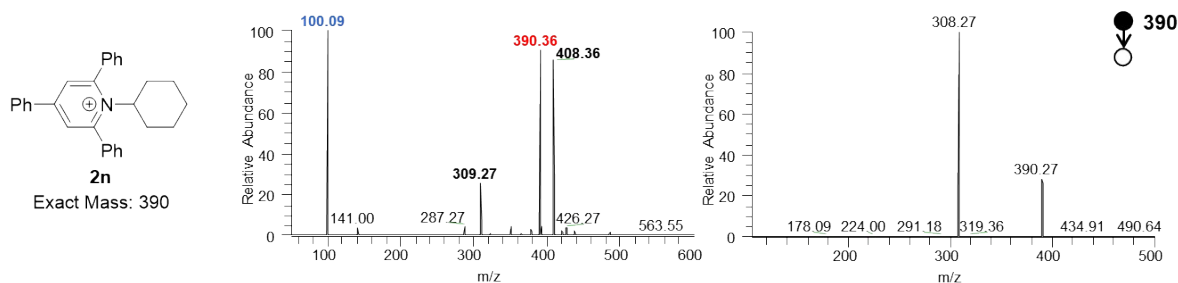
Figure S21. Mass spectrum illustrating the preparation of pyridinium **2l** under condition b (left panel). The signals for protonated amine **5l** and product **2l** are annotated in blue and red, respectively. The peaks at $m/z$ 309 and 380 represent TPP and addition product **6l**, respectively. The right panel shows the MS$^2$ spectrum of **2l** under CID 25. A zoomed spectrum (annotated in grey) is inserted.
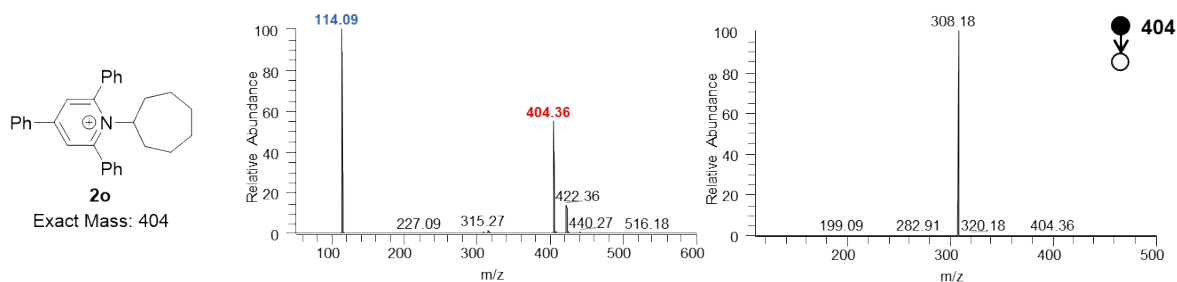


Figure S22. Mass spectrum illustrating the preparation of pyridinium **2m** under condition b (left panel). The signals for protonated amine **5m** and product **2m** are annotated in blue and red, respectively. The peaks at $m/z$ 309 and 394 represent TPP and addition product **6m**, respectively. The right panel shows the MS$^2$ spectrum of **2m** under CID 25.
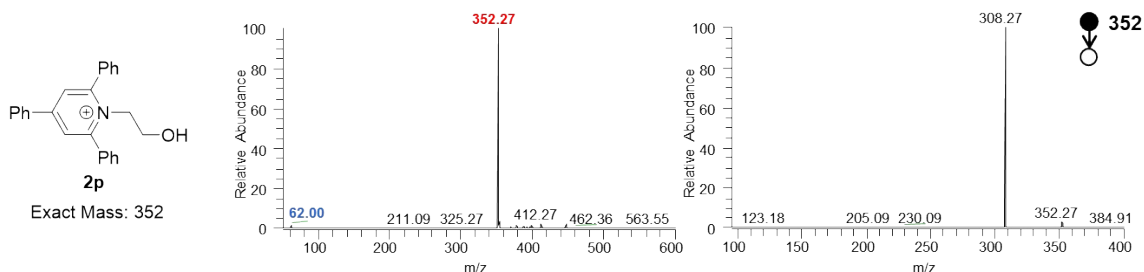


Figure S23. Mass spectrum illustrating the preparation of pyridinium **2n** under condition b (left panel). The signals for protonated amine **5n** and product **2n** are annotated in blue and red, respectively. The peaks at $m/z$ 309 and 408 represent TPP and addition product **6n**, respectively. The right panel shows the MS$^2$ spectrum of **2n** under CID 20.
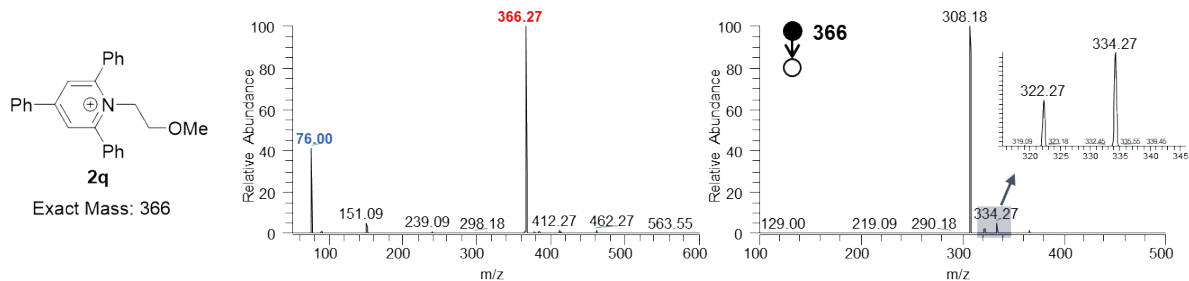
Figure S24. Mass spectrum illustrating the preparation of pyridinium **2o** under condition b (left panel). The signals for protonated amine **5o** and product **2o** are annotated in blue and red, respectively. The peak at *m/z* 422 represents addition product **6o**. The right panel shows the MS$^2$ spectrum of **2o** under CID 30.
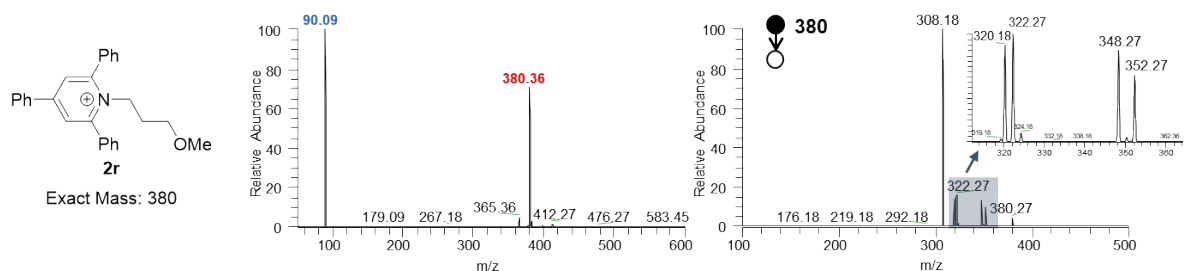


Figure S25. Mass spectrum illustrating the preparation of pyridinium **2p** under condition b (left panel). The signals for protonated amine **5p** and product **2p** are annotated in blue and red, respectively. The right panel shows the MS$^2$ spectrum of **2p** under CID 30.
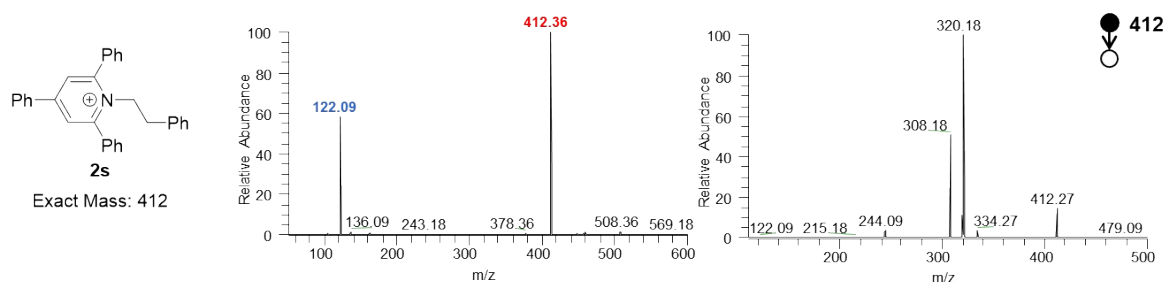


Figure S26. Mass spectrum illustrating the preparation of pyridinium **2q** under condition b (left panel). The signals for protonated amine **5q** and product **2q** are annotated in blue and red, respectively. The right panel shows the MS$^2$ spectrum of **2q** under CID 30. A zoomed spectrum (annotated in grey) is inserted.
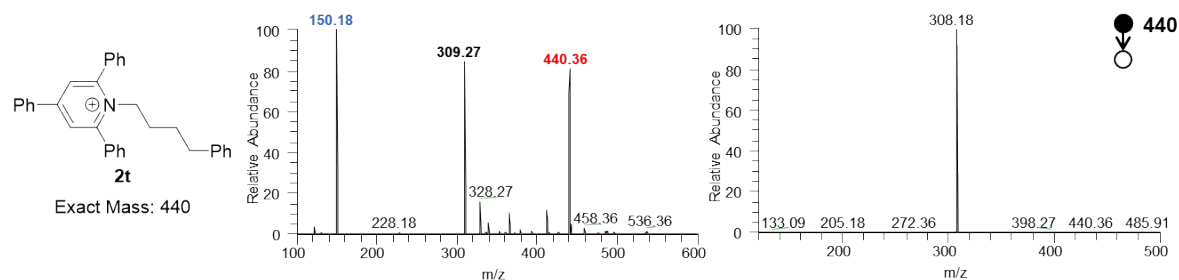
Figure S27. Mass spectrum illustrating the preparation of pyridinium **2r** under condition b (left panel). The signals for protonated amine **5r** and product **2r** are annotated in blue and red, respectively. The right panel shows the MS$^2$ spectrum of **2r** under CID 30. A zoomed spectrum (annotated in grey) is inserted.



Figure S28. Mass spectrum illustrating the preparation of pyridinium **2s** under condition b (left panel). The signals for protonated amine **5s** and product **2s** are annotated in blue and red, respectively. The right panel shows the MS$^2$ spectrum of **2s** under CID 35.
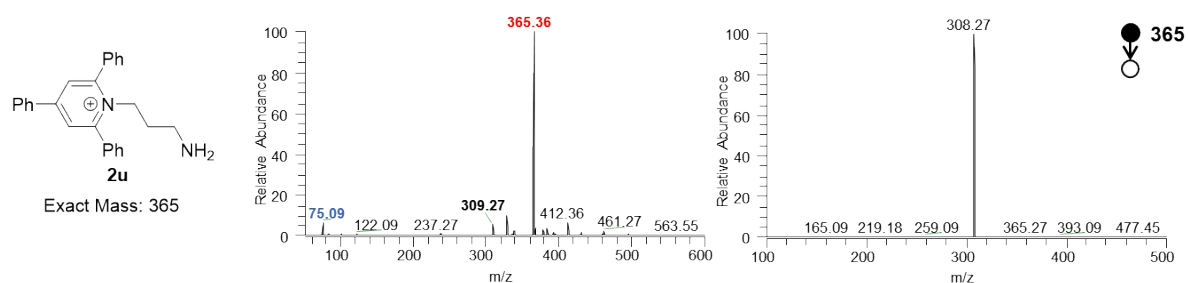


Figure S29. Mass spectrum illustrating the preparation of pyridinium **2t** under condition b (left panel). The signals for protonated amine **5t** and product **2t** are annotated in blue and red, respectively. The peak at *m/z* 309 represents TPP. The right panel shows the MS$^2$ spectrum of **2t** under CID 30.
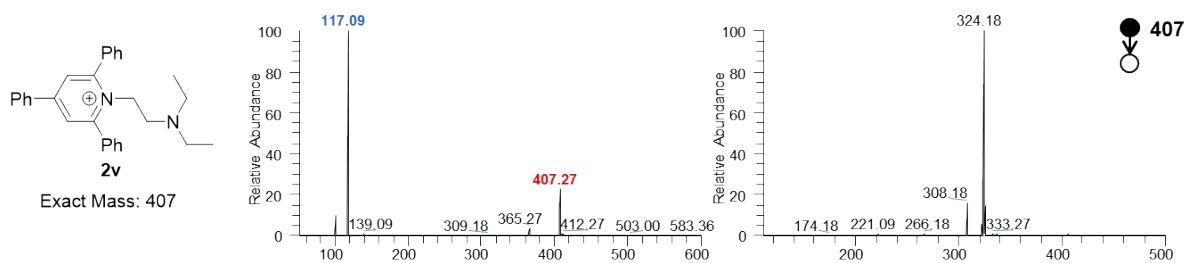
Figure S30. Mass spectrum illustrating the preparation of pyridinium **2u** under condition b (left panel). The signals for protonated amine **5u** and product **2u** are annotated in blue and red, respectively. The peak at *m/z* 309 represents TPP. The right panel shows the MS$^2$ spectrum of **2u** under CID 25.
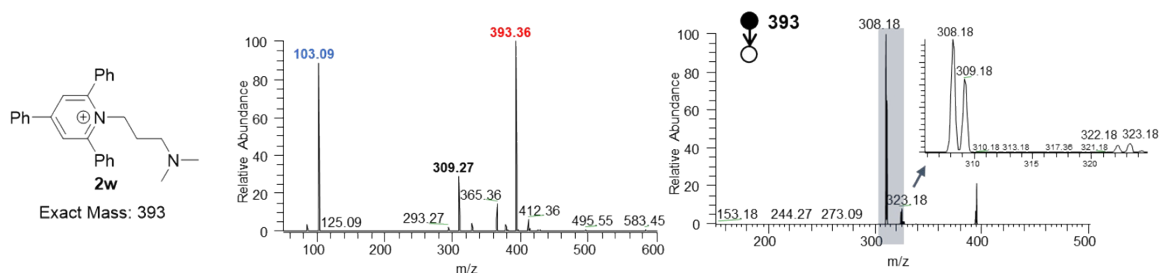


Figure S31. Mass spectrum illustrating the preparation of pyridinium **2v** under condition b (left panel). The signals for protonated amine **5v** and product **2v** are annotated in blue and red, respectively. The right panel shows the MS$^2$ spectrum of **2v** under CID 30.
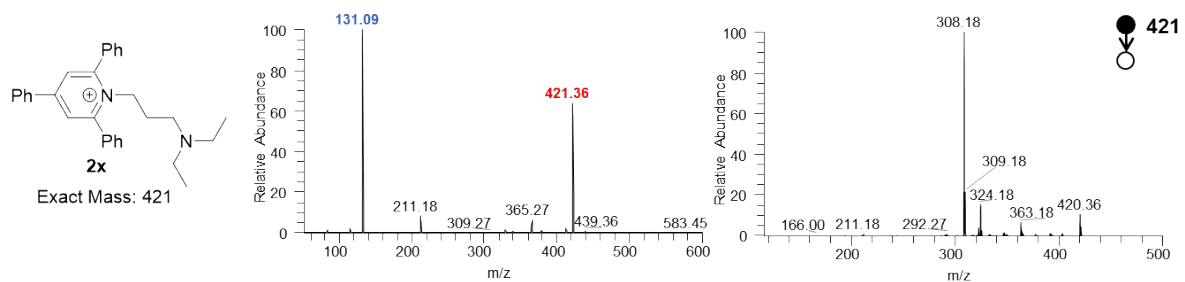


Figure S32. Mass spectrum illustrating the preparation of pyridinium **2w** under condition b (left panel). The signals for protonated amine **5w** and product **2w** are annotated in blue and red, respectively. The peak at *m/z* 309 represents TPP. The right panel shows the MS$^2$ spectrum of **2w** under CID 30. A zoomed spectrum (annotated in grey) is inserted.

Figure S33. Mass spectrum illustrating the preparation of pyridinium **2x** under condition b (left panel). The signals for protonated amine **5x** and product **2x** are annotated in blue and red, respectively. The right panel shows the MS$^2$ spectrum of **2x** under CID 25.
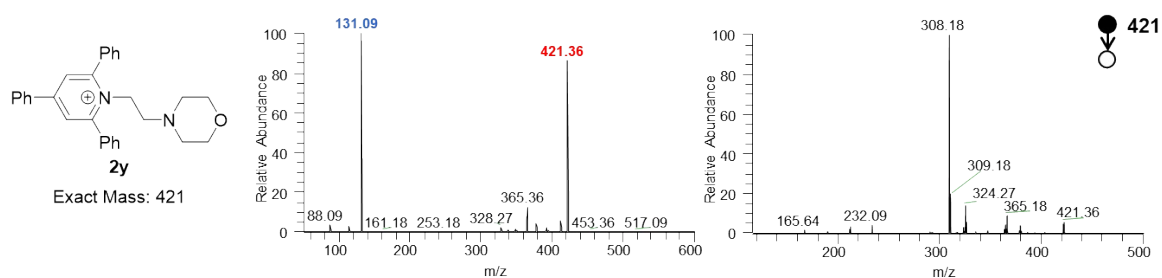


Figure S34. Mass spectrum illustrating the preparation of pyridinium **2y** under condition b (left panel). The signals for protonated amine **5y** and product **2y** are annotated in blue and red, respectively. The right panel shows the MS$^2$ spectrum of **2y** under CID 25.

## 4. Photocatalyzed amine oxidation via rapid, in-situ synthesis of pyridinium as photocatalyst

Two droplets, consisting of a reacting droplet containing 0.5 mM TPP solution (gold droplet in Fig. S35) and a n-octylamine droplet (blue droplet in Fig. S35), were deposited and trapped in the acoustic levitator. After a dosing time of one minute, the amine droplet was removed, and the reacting droplet was held in the levitator and exposed under 365 nm UV light for further reaction. After one minute, the entire reacting droplet was collected and diluted with 20 µL of acetonitrile for further detection. This sample was examined by nESI-MS analysis.



Step I. Droplet levitation     Step II. Vapor source removal     Step III. UV exposure     Step IV. Droplet collection
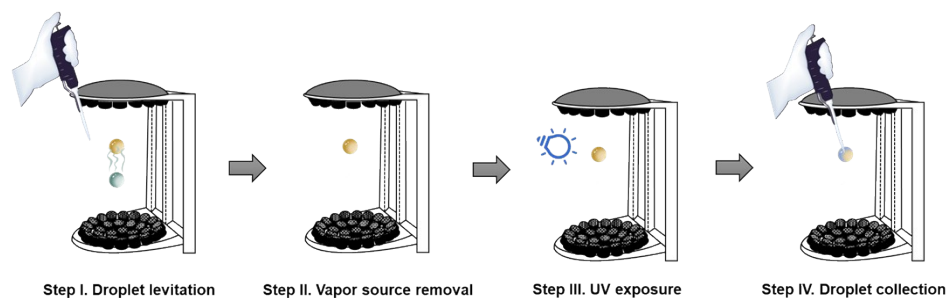
Figure S35. Illustrative process for photocatalytic amine oxidation mediated by in situ generated pyridinium
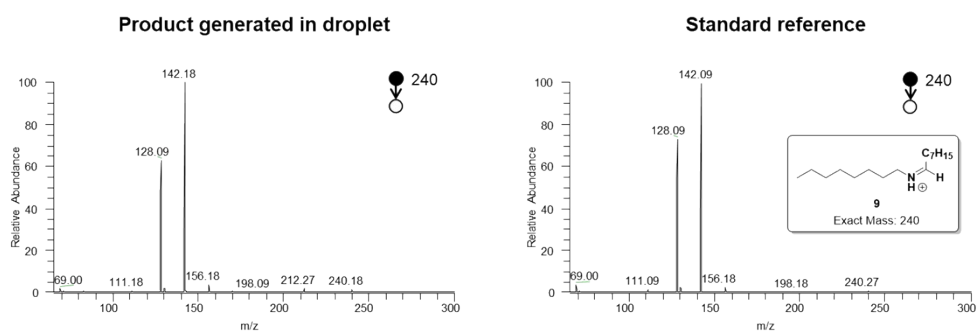


Figure S36. MS/MS analysis of the product of amine oxidation, **9**. The corresponding standard reference is shown on the right panel. This standard was prepared by mixing n-octylamine and n-octanal.
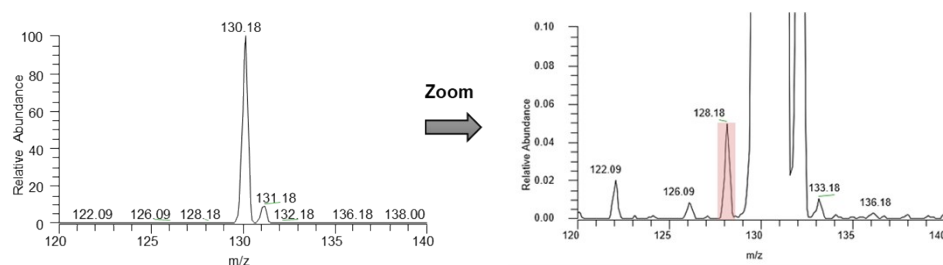


Figure S37. Detection of the direct oxidation product **7** at m/z 128. The base peak at 130 represents the signal of octylamine (mass 129).